


# Establishing Correlation Between Current and Voltage Signatures of the Arc and Weld Defects in GMAW Process

A. Sumesh<sup>1</sup>  · K. Rameshkumar<sup>1</sup> · A. Raja<sup>2</sup> · K. Mohandas<sup>1</sup> ·  
A. Santhakumari<sup>2</sup> · R. Shyambabu<sup>3</sup>

Received: 12 January 2016 / Accepted: 10 May 2017 / Published online: 23 May 2017  
© King Fahd University of Petroleum & Minerals 2017

**Abstract** Welding is one of the major metal-joining process employed in fabrication industries, especially in manufacturing of boilers and pressure vessels. Control of weld quality is very important for such industries considering the severe operating conditions. Industries are looking for some kind of real-time process monitoring/control that will ensure the weld quality online and prevent the occurrence of defects. In this paper an attempt is made to establish a correlation between the current and voltage signatures with the good weld and weld with porosity and burn through defect during the welding of carbon steel using gas metal arc welding (GMAW) process. Experimental setup has been established and experiments were conducted using a welding robot integrated with GMAW power source. The experimental setup includes online current and voltage sensors, data loggers, and signal processing hardware and software. Welding conditions are carefully designed to produce good weld and weld with defects such as burn through and porosity. Current and voltage signatures are captured using data acquisition system (DAS). Software has been developed to analyze the data captured by the DAS. Statistical methods are employed to study the transient data. The probability density distributions of the current and voltage signature demonstrates a good correspondence between the current and voltage signatures with the welding defect.

**Keywords** Current and voltage signature · Probability density distribution · Gas metal arc welding · Undisturbed arc · Disturbed arc

## 1 Introduction

In gas metal arc welding (GMAW), an electric arc is formed and maintained between a continuously fed consumable electrode wire and the weld pool. In the welding process, the consumable electrode wire is melted and transferred as droplets across the arc into the molten weld pool. The arc and the molten weld pool are protected from the atmospheric contamination by an externally supplied shielding gas.

Physics of welding is highly complex in nature which makes it difficult to develop a mathematical model to correlate the weld defects and welding process variables such as current, voltage, weld speed, stick out distance expressed by Martinussen [1]. Defects in welding are commonly classified as planar defects and Volumetric defect. In GMAW process, defects such as burn through, lack of fusion, porosity, and spatter are very common. The defects primarily focused in this work are burn through and porosity which occur frequently during the welding. The occurrence of these defects makes the welding arc unstable and hence will be reflected in the arc current and voltage. Defects like cracks and tears will not get reflected in the welding arc which motivated us to focus on burn through and porosity.

Many methods are reported in literatures to identify weld defects. Some of the methods are spectroscopic analysis, acoustic sensing, infrared sensing and electrical impedance method. In the spectroscopic analysis, radiation emitted by the plasma present in the electric arc is captured and analyzed to predict the weld quality [2–5].

✉ A. Sumesh  
a\_sumesh@cb.amrita.edu

<sup>1</sup> Department of Mechanical Engineering, Amrita School of Engineering, Amrita Vishwa Vidyapeetham, Amrita Nagar P.O, Coimbatore 641112, India

<sup>2</sup> Welding Research Institute, Bharat Heavy Electricals Ltd., Tiruchirappalli, India

<sup>3</sup> Best Oil & Gas Solution LLC, Muscat, Sultanate of Oman

Acoustic signals produced during the welding are used for monitoring the process and also for predicting the process stability and weld quality. Theoretical and experimental analysis of the acoustic signals has shown that welding arc sound represents the behavior of the electrical parameters of the welding arc. Pal [6], Cayo [7], Saini and Floyd [8], and Chen et al. [9] have investigated the use of arc sound as signature for quality monitoring of GMAW welding process.

The high temperature associated with the arc tends to cause strong spatial temperature gradients in the region of the weld pool. An infrared sensor can measure these temperatures by detecting the infrared energy emitted from the weld pool were reported by Nagarajan et al. [10], Wikle et al. [11], and Fan et al. [12].

Electro-optic sensors were used for monitoring of arc welding was employed by Sforza and Blasis [13] for the detection of visible, infrared, and ultraviolet emission of the plasma. A Fourier spectral analysis is used for identifying good and bad welds.

Electrical impedance characterizes a dynamic system and its variation with time reveals the conditions of the welding process. Waveforms of the real and imaginary part of the impedance directly reflect the thermomechanical behavior of the work pieces at the joining point. By recognizing the patterns of these waveforms, the weld joining quality was evaluated [14–16]. In their study, current and voltage sensors are used to determine the disturbances occurring in the GMAW process.

Wang and Chen [17] studied current voltage sensory information for plasma arc key hole welding. It is shown that the overall AC power of the arc signals, especially the low-frequency part ( $0 \pm 100$  Hz) of the arc signal power spectra, varies greatly with the variation of the status of the weld pool. Kang and Rhee [18] used current voltage sensors for studying the arc stability index of GMAW process. Eddy current sensors were used to determine subsurface flaws by McJunkin et al. [19]. Off late, current and voltage sensors are used for process optimization in GMAW 3D printing [20,21].

Anzehae and Haeri [22] developed a Markov-based model to control welding current and voltage. Molleda et al. [23] used Decision Support System (DSS) to assess the quality of resistance seam welds of steel strips by statistical analysis. Sathesh Kumar et al. [24] discussed the change in mechanical properties of GMAW and GTAW processes by changing the compositions of shielding gas. Zhang et al. [25] used the wavelet feature extraction from voltage signals to correlate the burn through for GTAW processes in welding of aluminum. Adolfsson et al. [26] developed a statistical change detection algorithm for determining the quality of weld in GMAW short circuit mode. From the literature review, it is found that for automating the welding process, online monitoring and control of the welding process are essential.

Current and voltage sensors were used to measure transient welding voltage and current signatures by Rehfeldt [27] and developed probability density distributions (PDD) for monitoring the welding process. Rehfeldt et al. [28–32] and Wu et al. [33–35] used PDD data for identifying weld defects using fuzzy c-means, neural network, and fuzzy Kohonen clustering networks. Kumar et al. [36] used self-organizing maps and neural networks for classification of quality of welders and compared with PDD.

Highly nonlinear nature of welding processes and lack of adequate models for predicting the weld defects are the fundamental motivations for this work. An attempt is made in this work to identify the weld defects using the PDD's generated using the current and voltage signals captured during the GMAW welding process.

In this work, welding trials were carried out to establish parameters for an undisturbed arc weld, and disturbances to the welding conditions were created in a control manner so as to induce porosity and burn through. Arc voltage and welding current were measured using low-pass filter and Hall effect sensors. TVC Arc Data logger is used for the acquisition of current and voltage signatures of GMA welding process.

A software is developed in this study for signal processing and data analysis. Transients and probability density distribution (PDD) were plotted with the help of this software. Transients and PDD's of defect free welds and weld with induced defects were compared to study the imprint of defects. The methodology adopted in this study is given below:

- Step 1* Establishing GMAW experimental setup
- Step 2* Experimental design (establishing conditions of good weld and weld with defects)
- Step 3* Conducting experiments (good weld conditions and welding process producing defects)
- Step 4* Capturing current and voltage signals using DAS
- Step 5* Signal processing
- Step 6* Plotting current and voltage PDD (for good weld and weld with defects)
- Step 7* Decision making

## 2 Experimental Design

Welding experiments are conducted using GMAW Industrial Robotic Welding System (IRWS). The important components of the IRWS includes arc robot, robot controller, control panel, power source, cooling system, dress package, wire feeder and RCU / KCP2 pendant. The robot used in this study for the experimentation is KUKA KR 16 robot. The important components of the IRWS are shown in Fig. 1. The important specification of the robot is given in Table 1. The robot is floor mounted and integrated with Fronius TPS-

**Fig. 1** KUKA KR 16—IRWS.  
1 Manipulator, 2 connecting  
cables, 3 robot controller,  
4 teach pendant

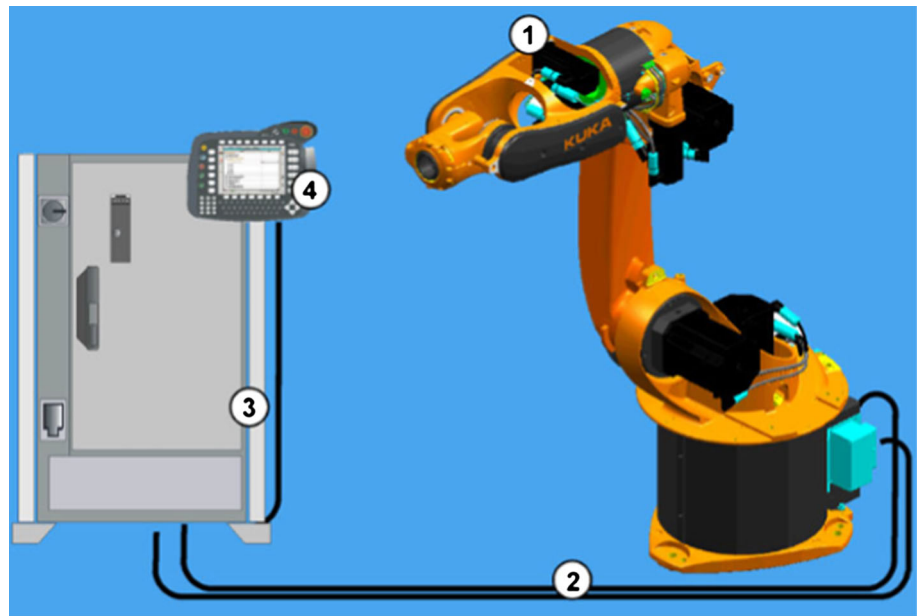


**Table 1** KUKA KR16 robot specification

S. No.	Specification	Details
1	Payload	16 kg
2	Work envelope—max reach	1636 mm
3	No. of axes	6
4	Weight	245 kg
5	Repeatability	$\pm 0.05$ mm
6	Weight	245 kg
7	Mounting position	Floor
8	Controller	KR C4
9	Protection class	IP 54

**Table 2** Specification of Fronius TPS-4000 power source

S. No.	Specification	Details
1	Mains voltage	$3 \times 400$ V
2	Voltage tolerance	$\pm 15\%$
3	Mains frequency	50/60 Hz
4	Primary continuous power	12.2 kVA
5	Welding current range	3–400 A
6	Duty cycle	50% DC at 400 A
7	Open-circuit voltage	70 V
8	Working voltage	14.2–34 V

4000 power source. The power source is fully digitized and microprocessor-controlled MIG/MAG power source for short circuit, spray and pulsed arcs which enables the best weld properties in every respect. Specification of the Fronius TPS-4000 power source is given in Table 2. Pulsed spray metal transfer, known by the acronym GMAW-P, was selected in this study for conducting the experiments. It is a highly controlled variant of axial spray transfer, which was developed to control the weld spatter and elimination of incomplete fusion defects common to globular and short-circuiting transfer. In GMAW-P, welding current is cycled between high peak current and a low background current. Metal transfer occurs during the high energy peak level in the form of a single molten droplet.

The current and voltage were captured using the commercially available data acquisition system; TVCALXII RS (portable model) manufactured by “The Validation Centre (TVC)”, UK. This system includes current sensor, volt-

age sensor and a data acquisition unit. The current sensor is a highly sensitive ‘Hall effect-type’ sensor which measures the axial magnetic field produced by the current in the wire. There is an error adjuster in the tong sensor to ensure there is no positive error displayed in the screen when the arc logger logs in. The arc voltage is measured between the electrode and the earth clamp by using a voltage sensor with a protection to high voltage. This data logger is a six-channel setup capable of capturing current, voltage, wire feed speed, travel speed and temperature signals. Weld data are captured at a maximum sampling frequency of 8 kHz. In this data logger the current can be measured in the range of 15–1999 A with an accuracy of  $\pm 2\%$  fsd and average voltage change from 0–99.9 V with an accuracy of  $\pm 1\%$  fsd. The portable type TVC arc logger is shown in Fig. 2.

Experimental setup used for conducting welding trials consisting of IWRS, gas mixing unit, welding torch, welding fixture, appropriate sensors for capturing the current and



**Fig. 2** TVC data logger (arc logger-ALXII)

voltage signals, and TVC data logger. The block diagram and photograph of the experimental setup is shown in Figs. 3 and 4, respectively.

**Fig. 3** Experimental setup

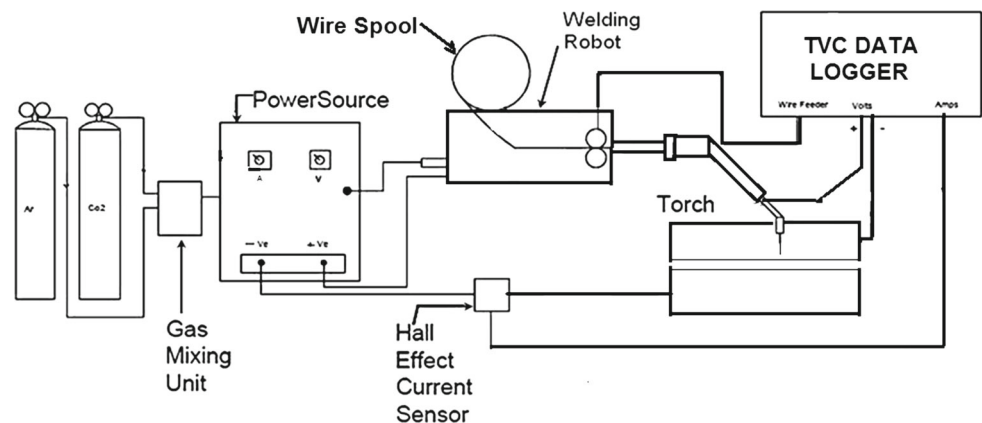


**Fig. 4** Photograph of the GMAW setup



In this study, linear welding is performed (i.e., lead through linear interpolation). Robot is taught by using two-point method. ‘KUKAArcTech Basic’ is the software package used for performing standard welding procedures. It expands the KUKA KR C4 controller and enables seamless communication with a weld power source. Robot has been integrated to Fronius power source synchronized with transynergic pulsed power. ‘KUKA ArcTech Basic’ gives the programmer all the necessary inline forms for programming the welding application. The robot programming components includes torch angle, wire feeder control, arc control, and gas flow control along with position control of the torch.

For shielding purpose, argon and carbon dioxide gas mixture is used in the ratio of 4:1 with a flow rate of 20 lpm using gas mixing unit. For all experiments, 12-mm-thick carbon steel plates are used. The weld joints were designed as ‘V’ groove butt joint with a groove angle of 70°. The wire diameter considered in this study for experimental purpose is 1.2 mm. Figure 5 shows the weld setup indicating weld fixture, torch, and weld specimen.



**Fig. 5** Photograph of welding setup

**Table 3** Good weld parameters

S. No.	Parameter	Details
1	Wire feed rate	3.5 m/min
2	Stick out distance	12 mm
3	Welding speed	30 cm/min
4	Gas flow rate	20 lpm
5	Wire diameter	1.2 mm
6	Groove angle	70°
7	Argon to carbon dioxide ratio	4:1

Good weld parameters were established by conducting experiments by following Welding Procedure Specifications (WPS) established by Welding Research Institute (WRI)—BHEL, Tiruchchirappalli, India. Experiments were carried out by varying wire feed rate, stick out distance and welding speed. The welding parameters for good weld were arrived by conducting welding trails in the shop floor by following WPS. Good weld parameters are shown in Table 3.

### 2.1 Experimental Design for Creating Good Weld and Weld with Defects

The main objective of this work is to establish correlation between the electrical parameters of the arc viz. welding current and voltage with two of the weld defects viz. porosity and burn through. Such correlation would help predicting the occurrence of the defect while welding operation in progress and corrective action could be initiated before damage is caused. The porosity and burn through defects are chosen for the study as they are greatly linked to the arc parameters. It is imperative to create the conditions for achieving good weld through undisturbed arc conditions and weld with specified defects through intentionally disturbed arc conditions. Arc conditions for good weld have been selected from the WPS and current and voltage signatures were captured for further analysis. Joint configurations and external disturbance have carefully designed and developed to create weld

with porosity and burn through. A ‘V’ groove butt joint weld geometry with 70° groove angle is designed for establishing good weld and weld with defects. Carbon steel plates of 12 mm thickness are used for the trials. For the good weld condition, weld geometry established in this study is shown in Fig. 6a. The photograph and RT image of the resultant good weld is shown in Fig. 6b, c, respectively.

### 2.2 Weld Condition for Occurrence of Burn Through Defects Through Joint Design

Experiments are carefully designed intentionally to create burn through defect in the weld joint. Burn through defect normally occur when the root gap goes beyond the process capability. Welding trials were carried out on a specially designed joint configuration (‘V’ groove butt joint having increasing root gap) as shown in Fig. 7. From these experiments, the burn through defect is found to occur at or beyond 1.3 mm root gap for zero root face, 2.3 mm root gap for 2.0 mm root face, and 3.6 mm root gap for 4.0 mm root face, respectively.

In the joints described above, the burn through defect will occur only once as the weld pool will collapse and the arc will extinguish with the root gap going beyond the tolerance limit of the process. However, it is required to have few number of burn through defects in the same test joint, in order to have large volume of data to be statistically significant. In order to have multiple burn through defects in the same joint, another kind of test joint has been designed as shown in Fig. 8. In this test joint, numbers of slots are machined at equal intervals along the joint. The dimensions of the slot are designed based on the results of various experiments. The slot length and width are also carefully designed so as to create burn through but at the same time not leading to the collapse of the weld pool or extinction of the arc. Slot width of 2 mm and length of 4 mm found to be suitable in our study for producing burn through defect. The weld pool and arc should be able to restabilize immediately after crossing the slot. This must be repeated with the encounter of every slot. This procedure helped to generate adequate quantum of data with least number of trials. It is to be noted that for producing defective weld (burn through and porosity), the parameters established for the good weld is used as reference for all other experiments which have been conducted to identify the defects viz. burn through and porosity. The photograph and RT image the resultant weld with burn through is shown in Fig. 9a, b.

### 2.3 Weld Conditions for Occurrence of Porosity Defect

Inadequate shielding gas coverage, contamination of weld surface by hydrocarbon substance, external wind disturbance, and absence of shielding gas are the likely causes for

**Fig. 6** a Good weld geometry.  
 b Photograph of the good weld.  
 c RT image of good weld

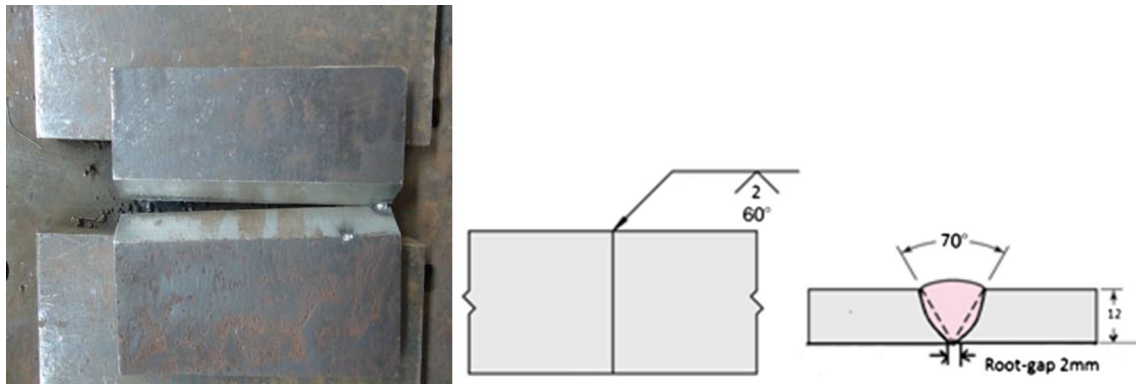
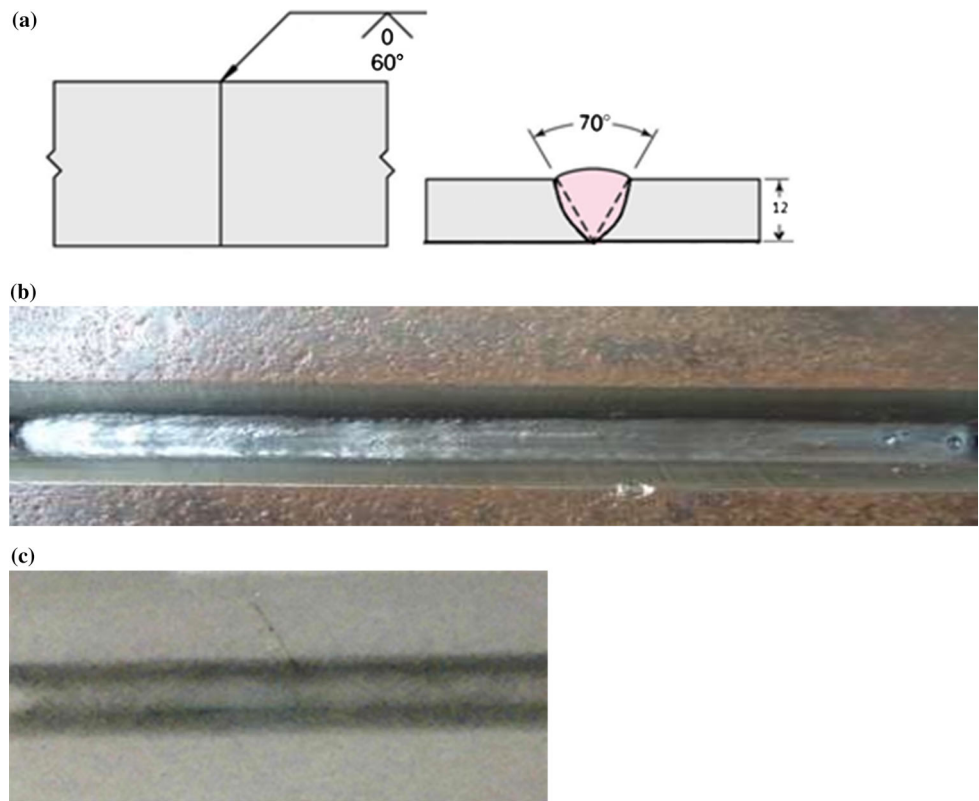


**Fig. 7** Weld specimen with increasing root gap for creating burn through defect

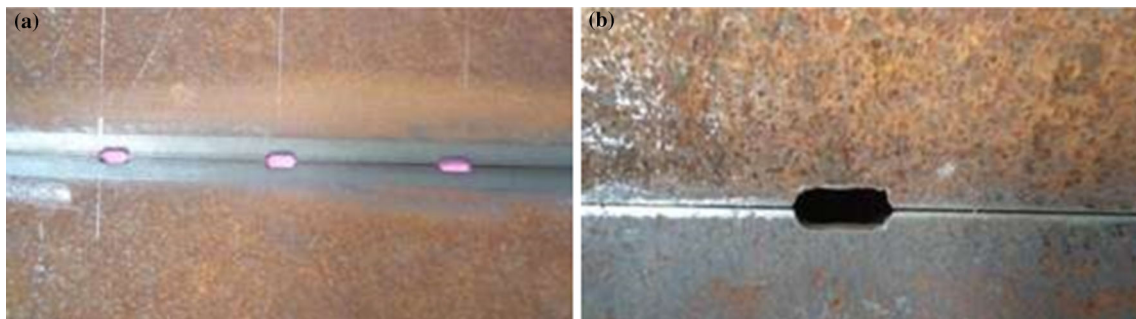


**Fig. 8** Joint design for burn through defect. a Slot design. b Slot enlarged view

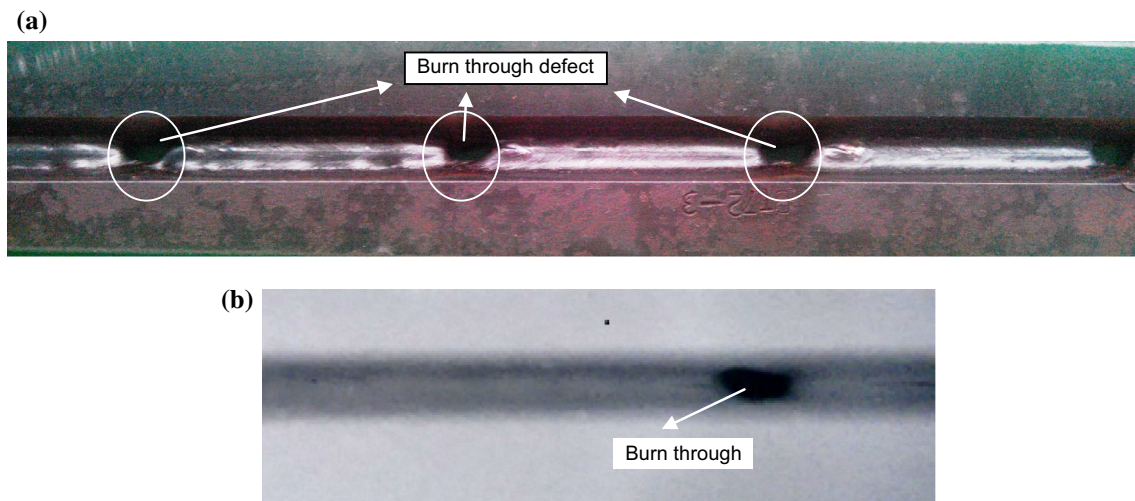


**Fig. 9** a Burn through weld specimen. b RT image of burn through welded specimen

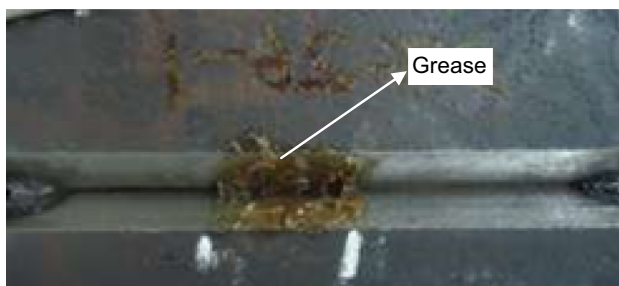


**Fig. 10** Weld specimen with grease



**Fig. 11** Resultant weld with porosity (Grease)

the porosity defect. Hence to introduce porosity in weld, two different disturbances were intentionally introduced in this study. One kind of disturbance is pre-placement of grease at specific locations along the weld joint and another kind is creating disturbance to shielding gas at periodic intervals by beaming compressed air through a hose positioned suitably. Figure 10 shows the weld surface with grease. Figure 11 shows the resultant weld with porosity. Figure 12a shows the experimental setup of beaming air over the shielding area resulting in reaction of atmospheric air with the arc thereby weld porosity is resulted. In this study, porosity in weld is also created by shielding gas cutoff. The resultant weld with

porosity is shown in Fig. 12b, and the RT image of the porosity weld is shown in Fig. 12c.

## 2.4 Experimental Studies

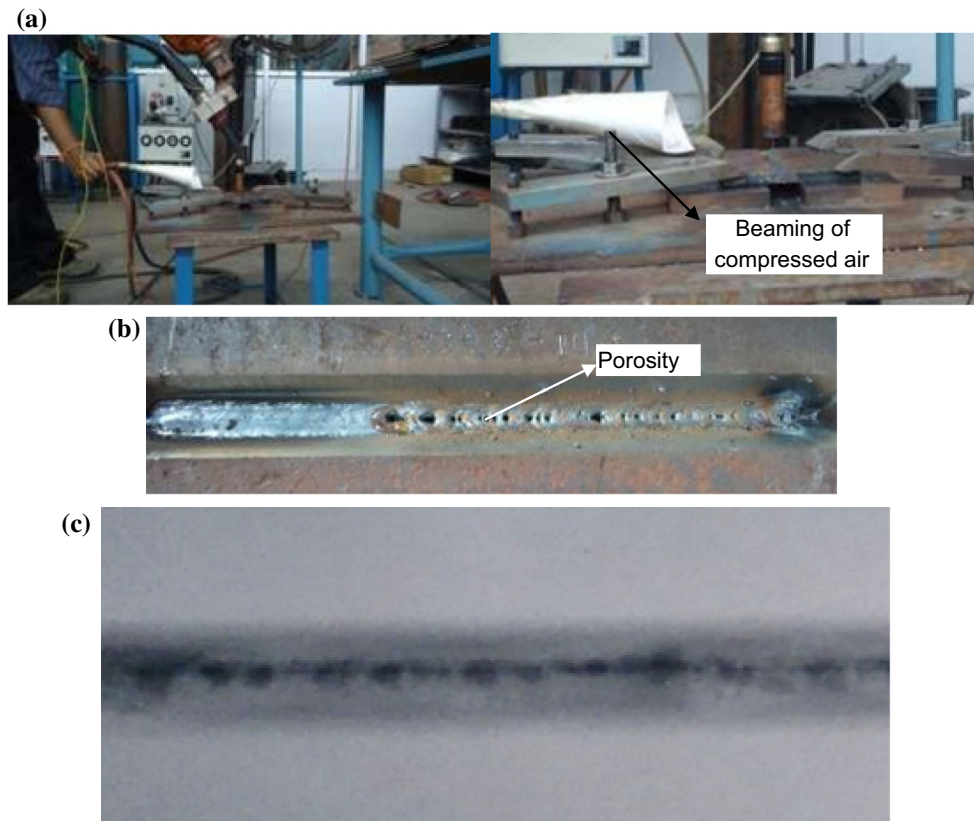
Experiments are conducted with good weld conditions and with experimental conditions created for achieving weld with porosity and burn through. During the welding process with varied weld conditions, current and voltage signals were captured and corresponding signals were recorded using the data logger. Welding trails were carried out using the good weld parameters as shown in Table 3. To ensure reputability of the experiments, five trials were carried out in each weld design for creating good weld and weld with porosity and burn through. For each of the experiments, weld qualities were tested using offline method to ensure repeatability of the experiments. The samples were inspected visually and as well as using RT images. In all the five repeated experiments for each weld design for good and defective welds, similar weld quality is achieved. This ensures the repeatability of experiments with the weld designs established in this study.

## 2.5 Signal Processing

Signal processing is done by using the TVC Arc Logger. The arc logger is having provision with an option for monitoring and analysis of pulsed welding process. During welding, arc logger can analyze each of the parameters, calculate, and display information on the pulse characteristics. It is also capable of recording and storing the data in the unit's hard drive. Acquired signal from the data acquisition system is in binary format.

The information recorded in data logger is used for data analysis. The data files are in .txt format and are converted

**Fig. 12** **a** Beaming of air from compressor. **b** Porosity weld shielding gas cutoff. **c** RT of porosity welded specimen with shielding gas cutoff



into transient plots. From the transient plots PDD's were obtained. A software using is developed to analyze the transients and plotting the current and voltage PDD's. For every experiment, average current, average voltage, peak current, and peak voltage is recorded in the data logger. These parameters are also calculated from the transients using the software developed in this study. These information's were cross-validated in order to ensure that there are no chances of errors in signal processing. For ensuring quality results, error in the signal processing is calculated using the relation shown in Eq. (1).

$$\text{Error\%} = \frac{\text{Actual average current, } I_{\text{avg}} - \text{Average current in data logger}}{\text{Actual average current, } I_{\text{avg}}} \times 100 \quad (1)$$

Average current,  $I_{\text{avg}}$ , for the current / voltage signature of the good weld as shown in Fig. 14 is calculated as follows:

$$I_{\text{avg}} = \frac{(I_p \times T_p) + (I_b \times T_b) + (I_s \times T_s)}{T_c} \quad (2)$$

where  $I_p$  is the peak current, 400 A;  $I_b$  is the background current, 32 A;  $I_s$  is the shoulder current, 200 A;  $T_p$  is the duration of the peak current, 0.001375 s;  $T_b$  is the duration of the

background current, 0.008 s;  $T_s$  is the duration of the shoulder current, 0.001375 s;  $T_c$  is the duration of one cycle, 0.01425 s

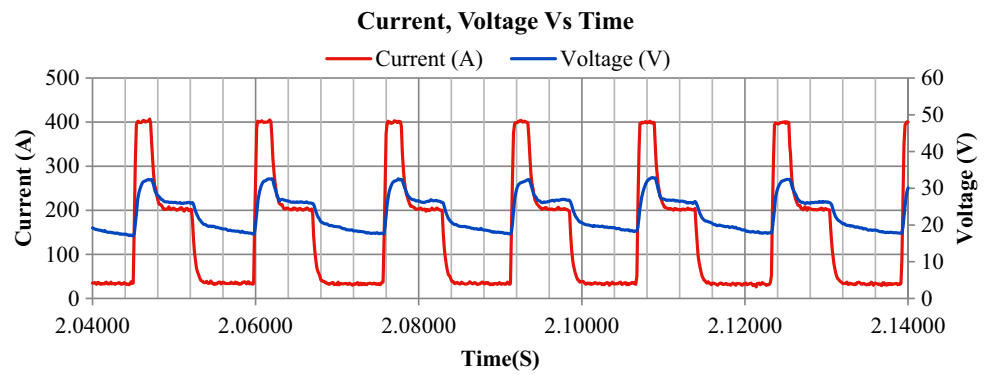
Substituting the parameters in Eq. (2),  $I_{\text{avg}}$  is found to be 124.98 A. Substituting  $I_{\text{avg}}$  in Eq. (1), the error works out to 3.18%, which appears to be low and well within the acceptable limit. Similarly for voltage signature, error is calculated. The peak voltage was found to be 29.5 V for a duration of 0.0025 S, the shoulder voltage of 24.5 for a duration of 0.00425 S and for a background current of 18.4 V the duration is 0.008 S. For one cycle the total duration will be 0.01425 s.  $V_{\text{Avg}}$  will be 21.77 V, and the DAC voltage is 22.4 V. The error (voltage) is 2.81%, which appears to be low and well within the acceptable limit.

### 3 Development of Probability Density Distribution (PDD) for Current and Voltage Signals

The current and voltage signatures are of highly stochastic in nature and therefore needs to be processed statistically. Hence an approach using the probability density distribution (PDD) is used to derive effective correlation between the transients of the current and voltage signals and weld defects. The PDD's give the summation effects of the current and voltage and is very effective in analyzing the raw data distributed in large masses. A procedure is established to



**Fig. 13** Current and voltage signature of the good weld



determine the PDD of current and voltage from the recorded transient data.

The basic method of determining the PDD is to distribute the frequency of the sampled values of the transient signals into different discrete classes [27,31,32]. The transient signal of welding current is captured and digitized while welding with the help of appropriate sensors and the acquisition system. The whole range of welding current is divided into 150 classes in the interval of 5 A starting from 0 A and a maximum of 750 A. Similarly, voltage is divided into 150 classes in the range 0 and 60 V. The number of measured current values in each class called frequency is determined.

A symbol defining a class such as 0.5–1.0 V is called the class interval. The difference between the lower and upper class limits is called class width. A class width of 0.4 V and 5 A is chosen for the development of PDD’s of voltage and current. The class width is selected based on the analysis of PDD’s of various class widths for its effectiveness in charactering the condition of the arc. Tabular arrangement of data by classes with corresponding class frequencies is called a frequency distribution or frequency table. The frequency of the class divided by the total frequency of all classes and is generally expressed as a percentage. This frequency distribution plotted in a histogram consists of a set of rectangles with centers at the class marks and widths equal to the class interval size and area proportional to class frequencies. The distribution of frequency values are of wide scale ranging from 0.000001 to .1, hence a semi-logarithmic scale is selected for plotting of PDD’s

### 3.1 Correlation Between Current and Voltage Signatures of Undisturbed Stable Arc Condition (Good Weld)

The undisturbed arc is characterized by the uniformity in the transients and the smoothness of the PDD’s of voltage and current. The transients of current and voltage for an undisturbed arc is shown in Fig. 13. The transient shows structure of the pulse waveform of the current and voltage. The waveform reveals three regions, namely peak current at 400 A,

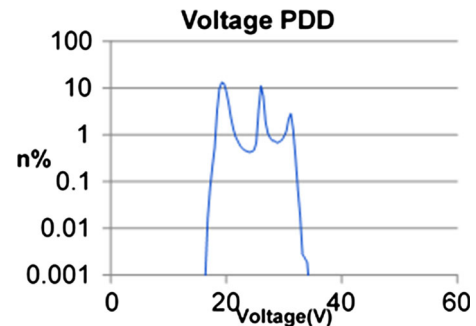


**Fig. 14** Voltage signature PDD of good weld

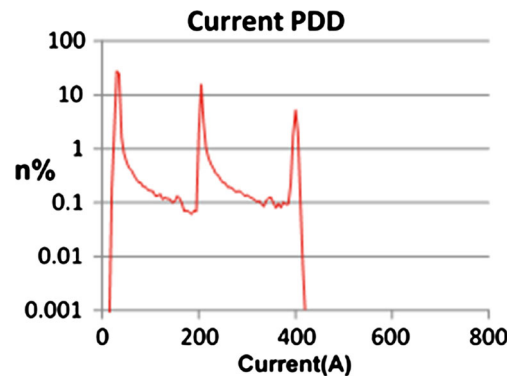


**Fig. 15** Current signature PDD of good weld

middle land or shoulder at 200 A, and back ground current at 50 A for the current waveform and similarly the voltage transients reveal peak voltage at 29.5 V, land or shoulder at 24.5 V and back ground voltage at 18.4 V in phase with the current waveform. These values are repeated cyclically. It is observed that for a good weld, PDD’s of current and voltage are having three peaks or modes and these three modes correspond to peak, shoulder, and background current as shown in Figs. 14 and 15, respectively. Current and voltage signatures of the good weld for the pulsed spray type of metal transfer obtained in this study is matching with the signatures reported in the literatures by Rehfeldt [32].

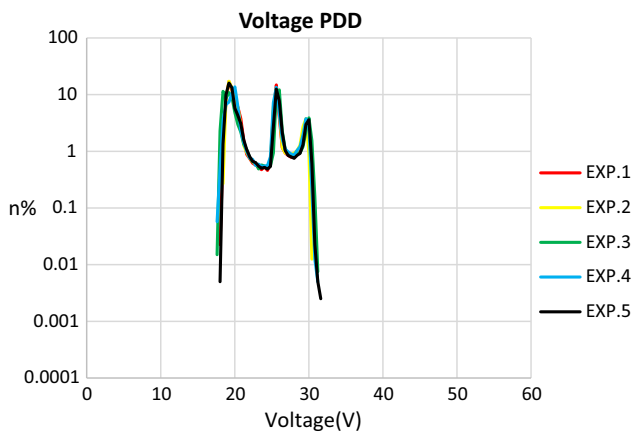


Fig. 16 Voltage PDD’s of repeatability trial for good welds

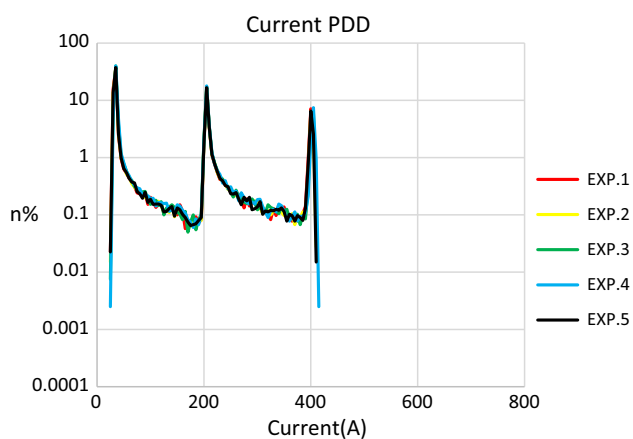


Fig. 17 Current PDD’s of repeatability trial for good welds

In order to check the consistency based on weld geometry, PDD’s were obtained by conducting five experimental trials for good weld conditions. PDD’s of all the trails were superimposed to the same scale for checking the consistency of the results. Current and voltage signature PDDs of the trials are shown in Figs. 16 and 17, respectively. All the five PDD’s of the current and voltage signatures are of similar pattern and consistent. Mean and standard deviation of average current, average voltage, peak current, and peak voltage of all the five experiments were computed and compared, since the average current, peak current, average voltage and peak voltage parameters determine the nature of PDD’s. The mean reflects the general amplitude of the measured variable—welding

voltage or current. The standard deviation demonstrates the difference between the values of stochastic variable. These statistic parameters are combined together to describe the dynamic and stochastic characteristics of a specific welding process. Statistical characteristic of a good weld is shown in Table 4.

### 3.2 Correlation Between Current and Voltage Signature with Burn Through Defect

In order to have multiple burn through defects in the specimen, slots are machined on the plates at equal intervals along the joint as per the procedure established in this study. The current and voltage transient of the burn through weld is shown in Fig. 18.

Current and voltage PDD’s were obtained by conducting experiments by using the welding parameters used for the good weld conditions for producing burn through defect in weld. Current and voltage signatures were captured by the arc logger and further processed and PDD’s were drawn using the software developed in this study. Current and voltage signature PDD’s of the trials are shown in the Figs. 19 and 20, respectively. All the five current and voltage PDD’s obtained with the repeated trails are superimposed in the same scale. The PDD’s of all the experiments are having similar pattern and consistent. This shows that there is a strong correlation between current and voltage signatures with the burn through defect.

In the current signature PDD of burn through weld, pulse structure is completely affected and the shoulder is disappeared as shown in Fig. 19. Due to the drop in voltage at the time of short circuiting, the voltage PDD shows the lower voltage (<10 V) which is not present in the case of undisturbed arc. There is a rise in the region near to 30 V in the case of burn through defect. Raise in voltage is taking place after the drop in voltage due to the short circuit. The shoulder is also flat which is also observed in the transient of the voltage signature shown in Fig. 20. The statistical characteristic of the burn through PDD is shown in Table 5. Peak current, average current, peak voltage, and average voltage of the five trials producing burn through defect was recorded. In order to verify the consistency of the PDD’s, mean and standard deviation of peak current, average current, peak voltage and average voltage of the PDD’s were computed. The results

Table 4 Statistical parameters of PDD’s of current and voltage signature—good weld

Parameter	Exp. 1	Exp. 2	Exp. 3	Exp. 4	Exp. 5	Mean	SD
Average current	127.59	135.86	132.23	128.30	126.87	130.17	3.39
Average voltage	22.45	22.66	22.45	22.40	22.40	22.47	0.09
Peak current	406	412	409	408	405	409	2.44
Peak voltage	31.50	32.60	31.00	30.20	30.60	31.18	0.83

**Fig. 18** Current and voltage transients of burn through weld

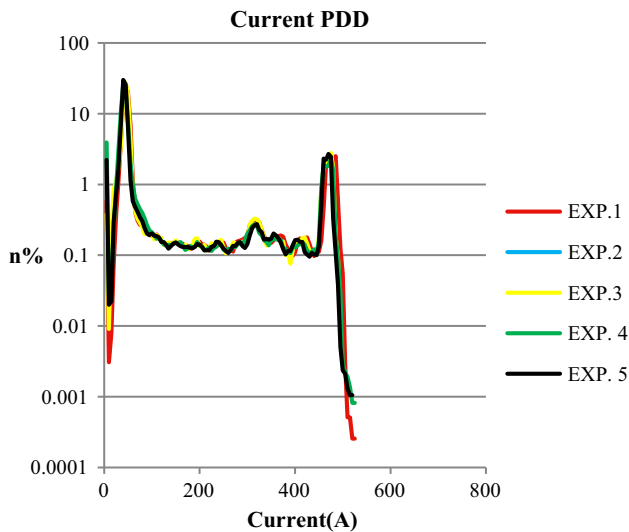
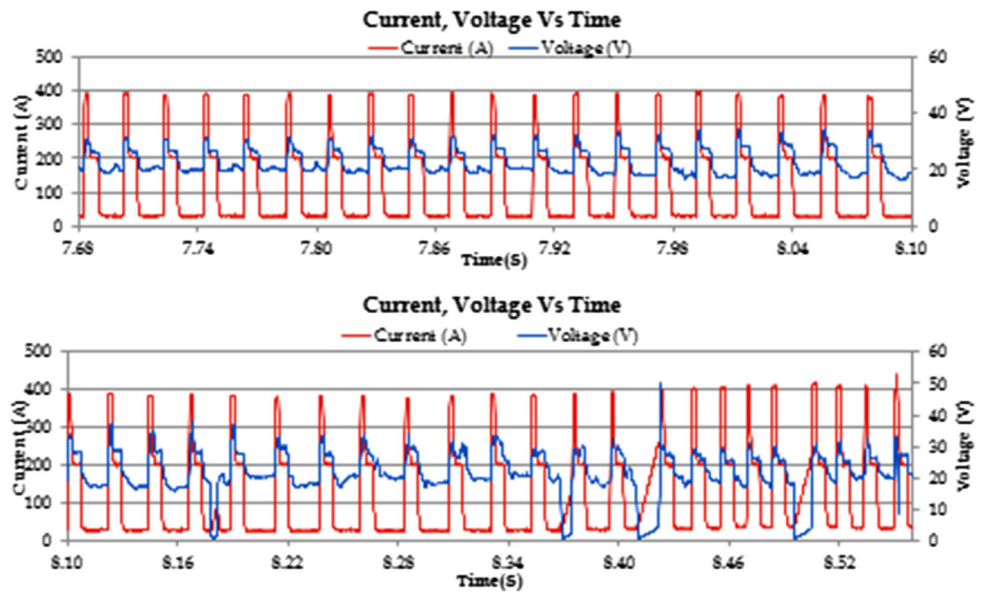


**Fig. 19** Current signature PDD's—burn through defect

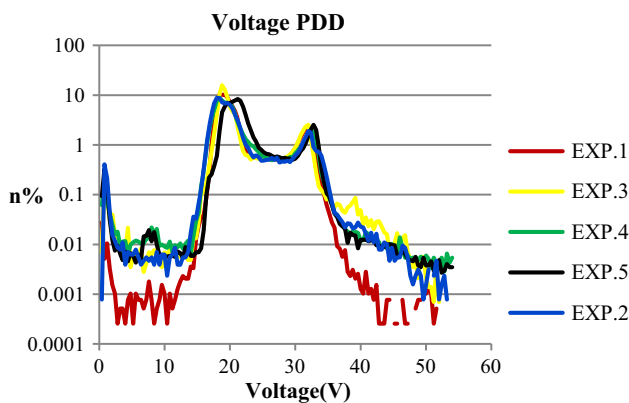


**Fig. 20** Voltage signature PDD's—burn through defect

indicate that there exists consistency in all the five experiments producing burn through defect. This also proves that repeatability of the experiments producing burn through. The outcome also validated using visual inspection and RT imaging.

### 3.3 Correlation Between Current and Voltage Signature with Porosity Defect

In GMAW Process the possible causes for porosity are absence of shielding gas, presence of oily substance on the groove and external wind disturbing the shielding gas. Under these conditions, the experiments were carried out and results are discussed.

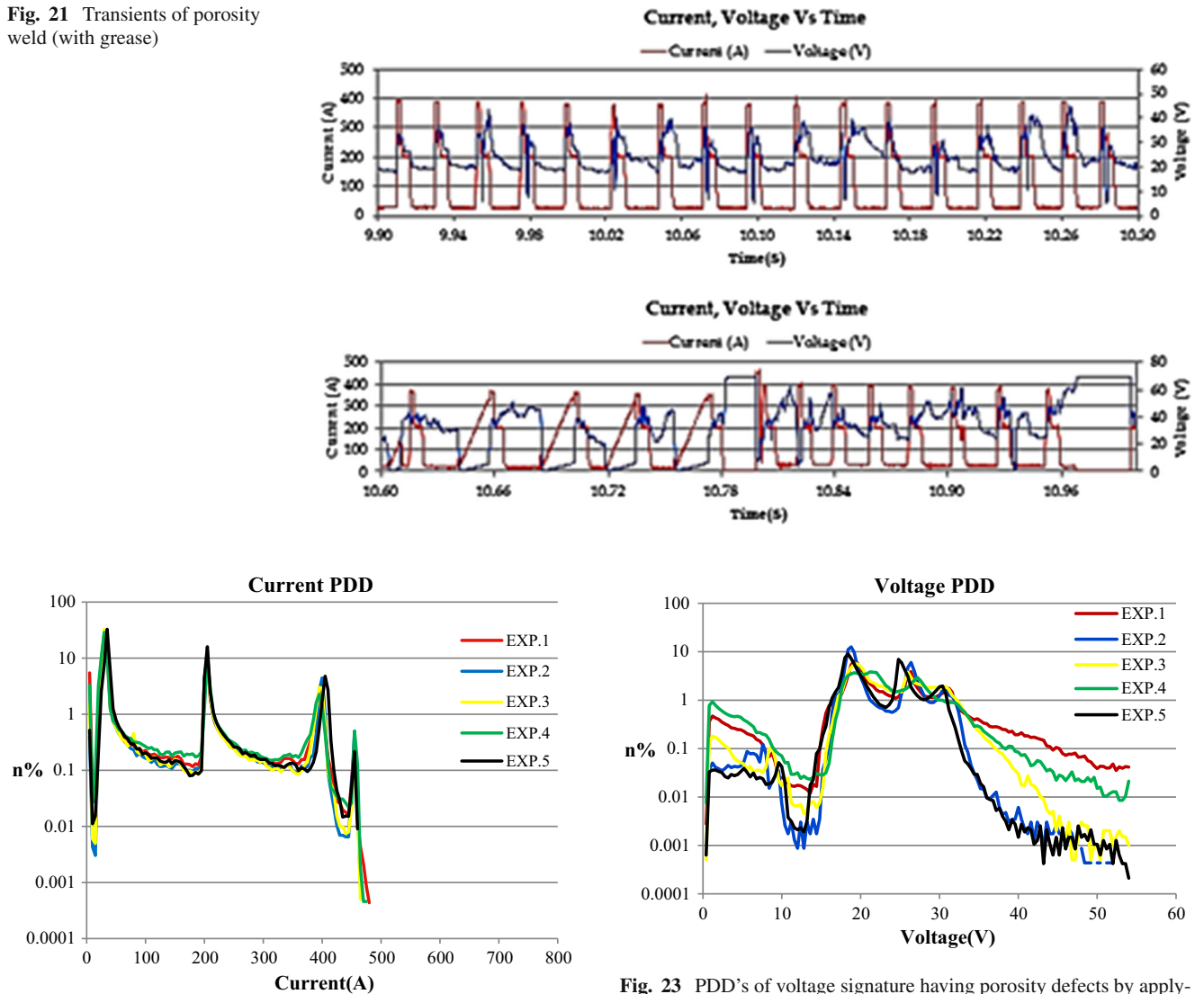
### 3.4 Application of Grease

Transients of porosity due to the presence of grease on weld groove are shown in Fig. 21. Transients show that the ramping current which is marked deviation from the undisturbed process. Instead of straight rising to the peak, current gradually rise to the peak, which results in the reduction in the duration of the peak current pulse. The same is reflected in the PDD of current in which the peak current is slightly lowered and shows the increase in the value of peak current and exceeds beyond 400 A.

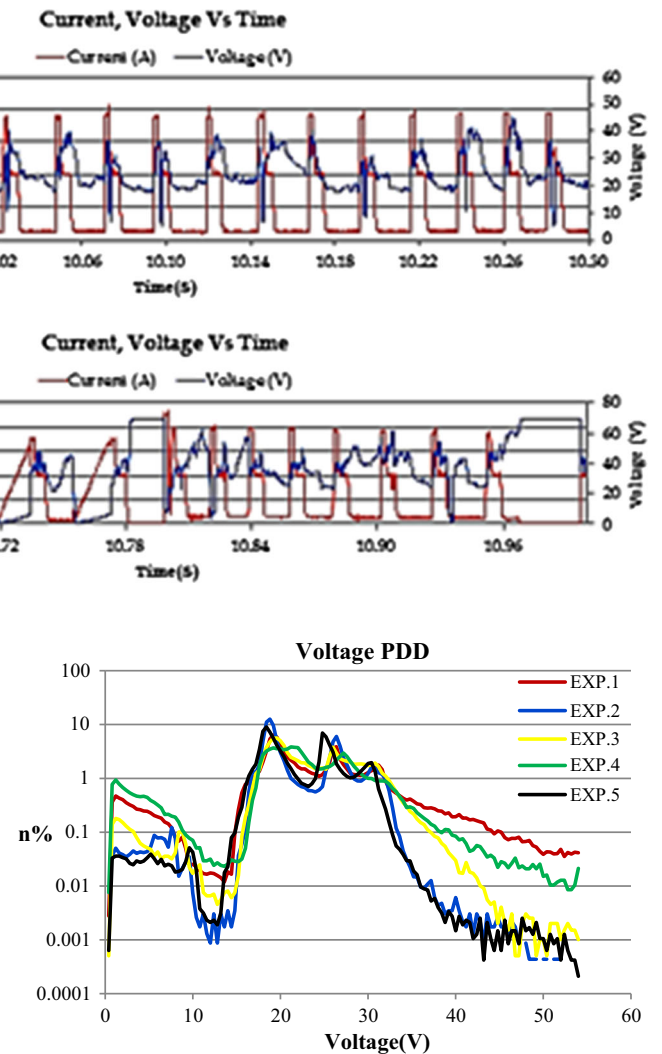
By comparing the porosity weld with good weld, it is observed that the voltage drops just before current start to rise as in the case of short-circuiting. The voltage increase to very high value (beyond 40V) than the undisturbed arc due to the reignition of the arc at higher voltage level. Current and voltage PDD's were drawn by conducting five experimental

**Table 5** Statistical parameters of PDD's of current and voltage signature—burn through defect

Parameter	Exp. 1	Exp. 2	Exp. 3	Exp. 4	Exp. 5	Mean	SD
Average current	118.11	120.81	109.56	109.49	110.03	113.60	5.44
Average voltage	21.69	21.69	21.50	23.45	23.69	22.40	1.07
Peak current	507	534	517	524	518	520	9.92
Peak voltage	71.20	74.40	71.10	84.10	75.30	75.22	5.31

**Fig. 21** Transients of porosity weld (with grease)**Fig. 22** PDD's of current signature having porosity defects by applying grease

trials with the same welding conditions for producing porosity weld. PDD's of all the trails were drawn to the same scale for checking the consistency of the results. PDD plots of the trials are shown in Figs. 22 and 23. All the five PDD's of the current and voltage signatures are of similar pattern and consistent. This shows there is a strong correlation between current and voltage signatures with the porosity defect. Mean and standard deviation of average current, average voltage, peak current, and peak voltage of all the five experiments

**Fig. 23** PDD's of voltage signature having porosity defects by applying grease

were calculated and compared and are shown in Table 6. The results indicate that there exists consistency in all the five experiments producing burn-porosity defect with the application of grease. The outcome also was validated using visual inspection, and RT imaging shows the repeatability of experiments. Voltage PDD has a flat region on the top and between 18 and 30 V, instead of three peaks. Voltage PDD also shows the lower value which indicates the drop in the voltage during the shorting time and spread beyond 40 V due to the reignition at higher voltage level.

**Table 6** Statistical parameters of PDD’s of current and voltage signature—Porosity defects by applying grease

Parameter	Exp. 1	Exp. 2	Exp. 3	Exp. 4	Exp. 5	Mean	SD
Average current	112.19	120.16	116.12	113.28	134.94	119.34	9.25
Average voltage	26.00	22.24	24.09	23.46	22.21	23.60	1.57
Peak current	477	477	465	472	478	473.8	5.45
Peak voltage	70	69.9	71.2	70.9	67.5	69.9	1.45

### 3.5 Shielding Gas Cutoff

Shielding gas was totally removed once the arc was stabilized after ignition to induce porosity in the weld bead. Transients of current and voltage are shown in Fig. 24. Current and voltage PDD plots of the trials are shown in Figs. 25 and 26, respectively. All the five PDD’s of the current and voltage signatures are of similar pattern and consistent. This shows there is a strong correlation between current and voltage signatures with the porosity defect with gas cutoff. Mean and standard deviation of average current, average voltage, peak current, and peak voltage of all the five experiments were calculated and compared and are shown in Table 7.

While comparing the porosity created due to the presence of grease, ramping current associated with the drop in the arc voltage is observed in the case of shielding gas cutoff. This ramping current associated with the drop in the arc voltage indicates the signature of porosity. The PDD’s of the voltage shows the voltage in the lower level indicating the short circuiting and the spread beyond 50 V indicating the reignition of arc at higher voltage levels. PDD’s of current shows a forth

**Fig. 24** Transients of porosity weld shielding gas cut-off

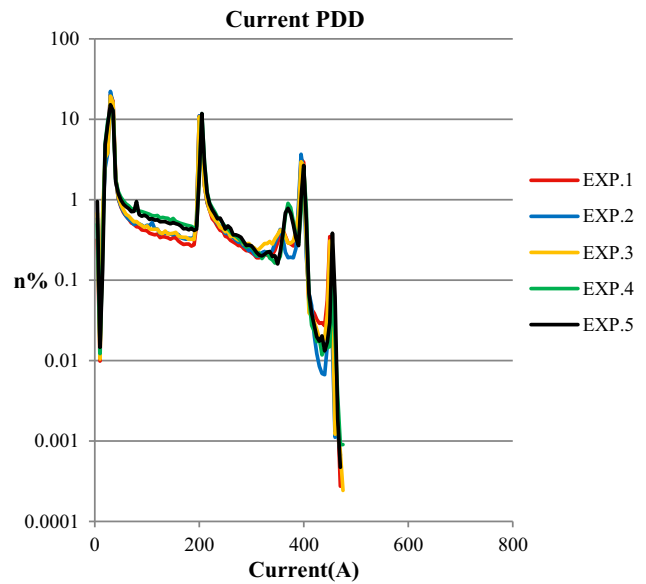
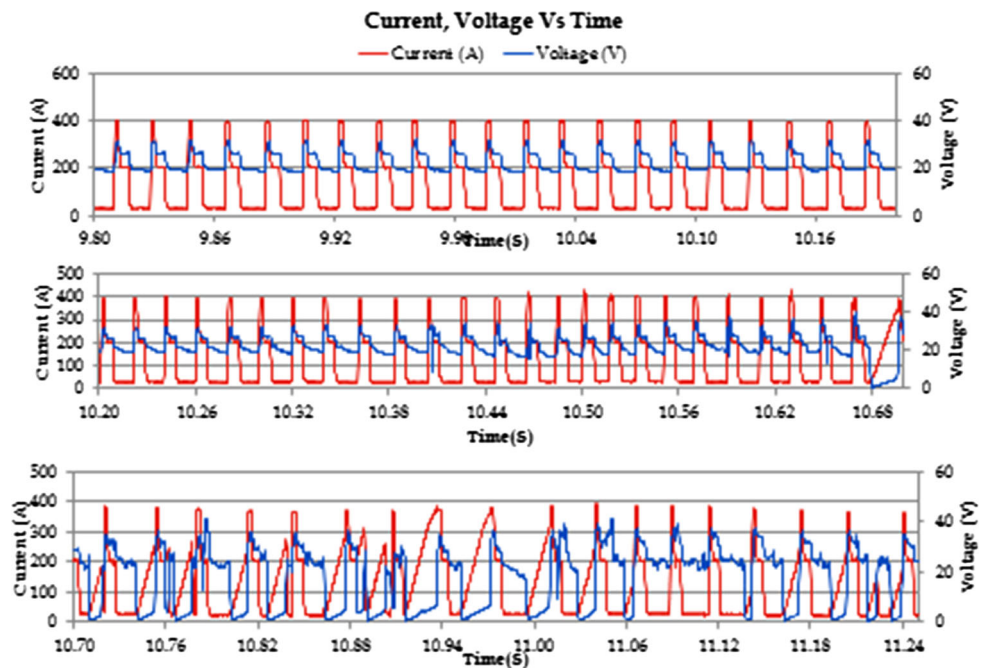


**Fig. 25** PDD’s of current signature having porosity defects—gas cut-off

peak which is at very high level (450 A) than the normal peak current.

### 3.6 Beaming the Air

The shielding of weld arc was disturbed with the beaming of air from compressor to induce porosity in the weld bead. Similar to previous two cases transients shows the ramping current and associated drop in the arc voltage which is the main feature for the identification of porosity. Transients of

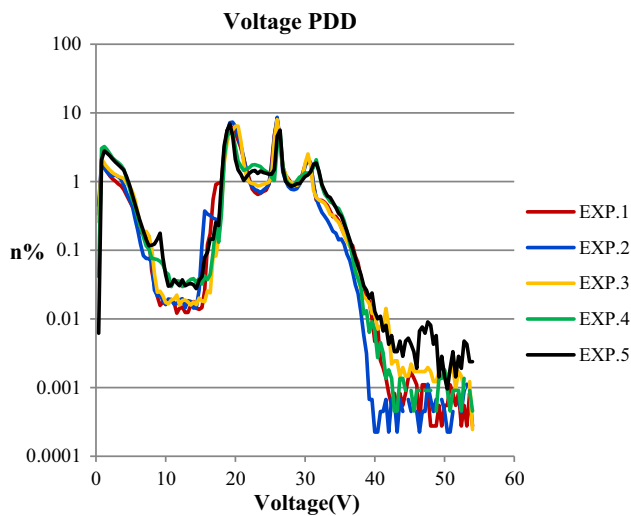


**Fig. 26** PDD's of voltage signature having porosity defects—gas cut-off

current and voltage are shown in Fig. 27. PDD's of current and voltage for the five trials with same weld conditions are shown in Figs. 28 and 29, respectively. All the five PDD's of the current and voltage signatures are of similar pattern and consistent. This shows there is a strong correlation between current and voltage signatures with the porosity defect with beaming of air. Mean and standard deviation of average current, average voltage, peak current, and peak voltage of all the five experiments were calculated and compared and are shown in Table 8.

## 4 Comparison of PDD's of Good Weld with Defective Welds

### 4.1 Comparison of PDD's Good Weld with Weld with Porosity Defect

The PDD's of current/voltage obtained for porosity defect caused due to the presence of grease [PG], absence of shielding gas [PL], and external disturbance [PA] to the shielding by compressed air are compared and shown in Fig. 30a, b to study its specific imprint on the PDD's of current voltage signals. From the figure, it is clear that there is a similarity in the three types of porosity welds, vice PG-weld (contamina-

tion of weld groove by grease), PA-weld (disturbance in the shielding due to introduction of compressor air), and PS-weld (lack of shielding gas).

The PDD's of current and voltage of the disturbed arc very much deviate from the PDD's of undisturbed arc. It is evident from voltage PDD that there is a low voltage region due to short circuiting caused by the disturbance (which normally not expected in pulsed spray process) and very high voltage regions due to the reignition after short circuiting at higher voltage levels. In the case of current PDD, the smoothness in the curve of undisturbed process is not seen in the case of disturbed process. For the weld with contamination, there is fourth peak in the PDD indicating the rise in the peak current to above 450 A in the signature of the porosity weld. These deviating features in the PDD's of current/voltage are significant and could be the features indicating the onset of porosity defect. From the transients of current and voltage signatures, it is observed that current is rising above 400 A and voltage dropping to zero during the occurrence of porosity, which is in correspondence with the PDD's.

### 4.2 Comparison of Good Weld with Burn Through and Porosity Weld

To study the pattern and recognize the difference in PDD's of burn through and porosity PDD's of undisturbed weld, weld with burn through, weld with porosity due to contamination of welding groove, and porosity due to the lack of shielding gas are compared and are shown in Fig. 31a, b.

It can be observed that voltage PDD of both the porosity segment shows distribution in lower level and higher (above 40 V) levels of voltage. It is noticed that there is a short-circuiting region and arc reignition at higher voltage levels (above 40V), when porosity is being developed.

PDD of BT is much different from that PDD of the porosity weld, though there is a voltage distribution in the lower range is very narrow and completely different form that of porosity. In the current PDD, there exists a fourth Peak which does not exist in burn through signature. From the variations in the PDD's, it is possible to distinguish good weld from weld with porosity and burn through. PDD's pattern of the weld with burn through and porosity are unique and one can clearly distinguish the type of defect by investigating the PDD.

**Table 7** Statistical parameters of PDD's of current and voltage signature—porosity defects by gas cutoff

Parameter	Exp. 1	Exp. 2	Exp. 3	Exp. 4	Exp. 5	Mean	SD
Average current	130.48	129.42	132.88	132.99	128.18	130.79	2.12
Average voltage	20.77	20.45	20.42	20.77	18.99	20.28	0.74
Peak current	466	492	473	482	471	476.8	10.28
Peak voltage	69.3	69.7	69.7	69.9	65.5	68.82	1.86

**Fig. 27** Transients of porosity weld beaming of air

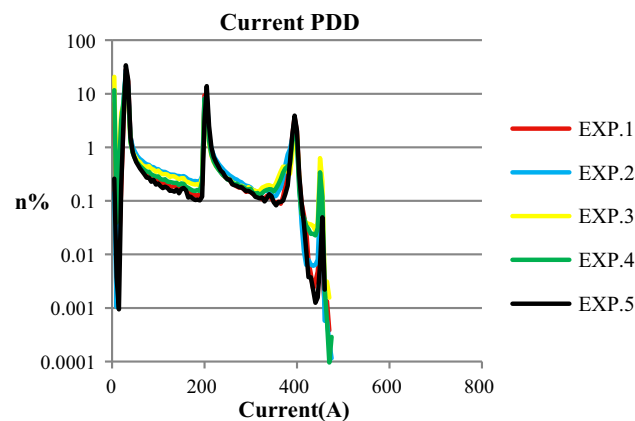
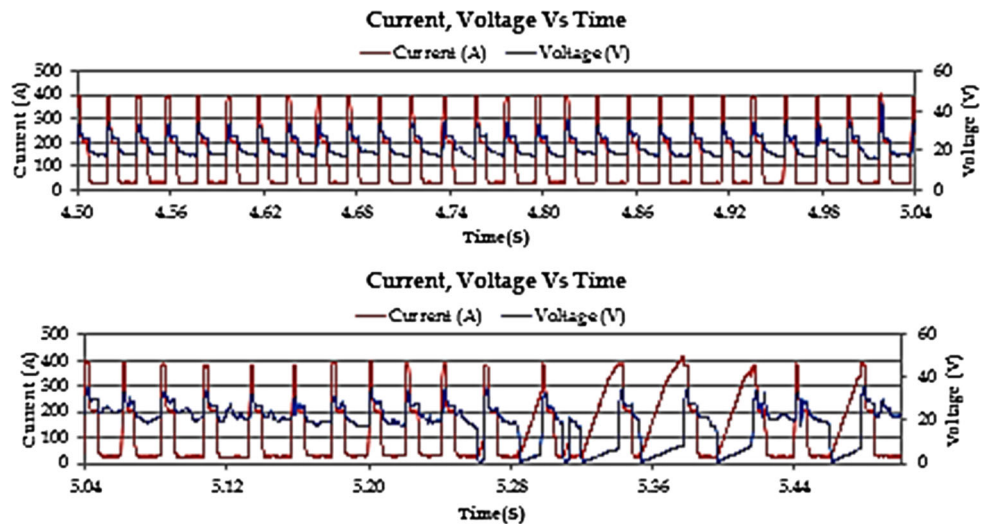


**Fig. 28** PDD's of current signature having porosity defect beaming the air

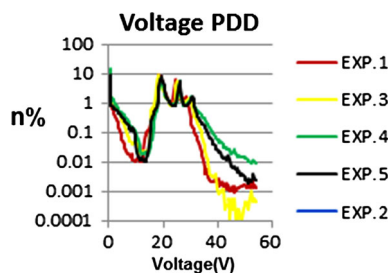


**Fig. 29** PDD's of voltage signature having porosity defect beaming the air

From Tables 5, 6, 7 and 8, it is noted that the average current value of the weld with burn through and porosity reduces when compared with good weld. At the same time, average voltage remains same in both the cases. During the burn through process, short circuiting, reigniting of arc will take place which raises the peak current and voltage when compared to the undisturbed process. This has been reflected in the PDD. For the weld with porosity, there exists a fourth

peak in all the PDD's of current signature. The fourth peak is due to the conditions induced for creating the defect.

### 4.3 Application Limits of the Established Correlation and Feature Scope

Current and voltage PDD's possibly can be used as a fingerprint to identify the weld defects. Repeatability of good weld and defective welds were achieved for the weld designs established in this study. For the given type of material, joint design, thickness of the joining plates, gas flow rate and root gap, the results provided in the study are valid and the experiments are repeatable.

In this study, a correlation established between current and voltage PDD's and weld defects for GMAW process with pulse spray metal transfer mechanism. Further studies can be carried out in other metal transfer mechanisms such as short circuit, globular, surface tension transfer. Two types of weld defects namely burn through and porosity were considered in this study. Other weld defects such as spatter, lack of fusion, etc., have to be studied further. In this study, experiments were conducted using 'V' joint type of configuration. By varying thickness of the plate, other joint configurations also can be studied. High-speed data acquisition systems can be utilized for capturing current and voltage signatures for establishing real-time weld quality monitoring system.

## 5 Conclusion

In this paper, an attempt has been made to establish a correlation between the current and voltage signatures and two types of weld defects viz. porosity and burn through. Experiments were conducted on carbon steel plates using an industrial robotic welding system (IRWS) integrated with GMAW power source. Experimental conditions were estab-

**Table 8** Statistical parameters of PDD's of current and voltage signature—Porosity defects by beaming the air

Parameter	Exp. 1	Exp. 2	Exp. 3	Exp. 4	Exp. 5	Mean	SD
Average Current	114.38	121.89	101.67	107.3403	117.23	112.50	8.03
Average Voltage	21.18	19.79	21.17	20.61	22.27	21.01	0.90
Peak Current	468	471	470	475	467	470.2	3.11
Peak Voltage	69.3	67.3	69.5	69.5	69.9	69.1	1.02

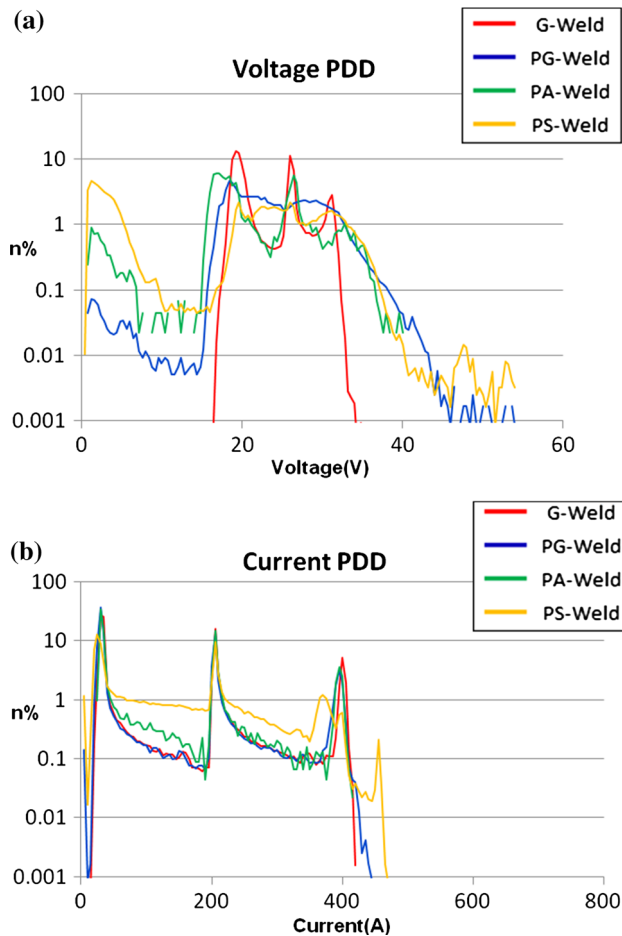


**Fig. 30** **a** Comparison of voltage signature PDD of good weld with porosity weld. **b** Comparison of current signature PDD of good weld with porosity weld

lished to intentionally create weld with porosity and burn through defects. Welding conditions were carefully selected to produce undisturbed arc to produce good weld and weld with burn through and porosity in a controlled manner.

Current and voltage signals were captured using data acquisition system for the experimental conditions producing good weld and weld with porosity and burn through. Software has been developed for processing and analysis of raw data captured by data acquisition system. Statistical method was employed to study the transient data and current and voltage PDD's for establishing correlation between arc signature and weld condition.

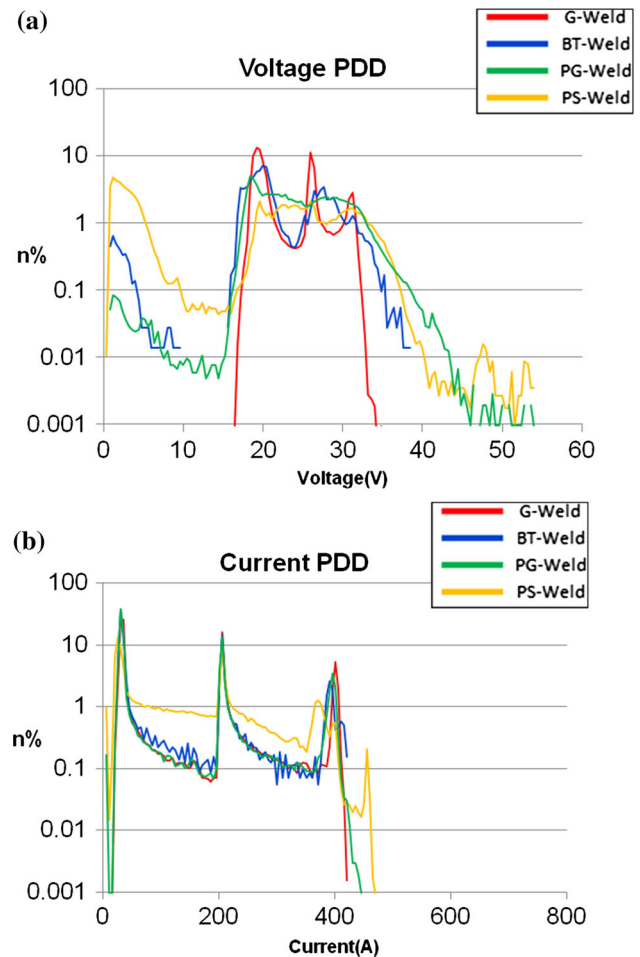


**Fig. 31** **a** Comparison of voltage PDD of good weld with defective welds. **b** Comparison of current PDD of good weld with defective welds

From the current and voltage PDD's, it is observed that there is a strong correlation existing between current and voltage PDDs with that of the welding defect. It is evident that the current and voltage PDD's of disturbed process (disturbances causing porosity or burn through defects) significantly deviate from the PDD's of undisturbed process. Confirmatory tests are also proved that similar patterns were achieved during the welding. These deviating features could be used as an indicator of the onset of the porosity and burn through defect.



**Acknowledgements** Authors acknowledge their sincere thanks to M/s Welding Research Institute (WRI)—BHEL, Tiruchirappali, India, for using their facility for conducting welding trails. Authors also acknowledge their sincere thanks to the reviews for their useful comments and suggestions for improving the quality of the paper.

## References

- Martinussen, M.: Numerical modelling and model reduction of heat flow in robotic welding. Master Thesis, Norwegian University of Science and Technology (2007)
- Mirapeix, J.; García-Allende, P.B.; Cobo, A.; Conde, O.M.; López-Higuera, J.M.: Real-time arc-welding defect detection and classification with principal component analysis and artificial neural networks. *Int. J. Non Destr. Test. Eval.* **40**, 315–323 (2007)
- Zhiyong, L.; Bao, W.; Jingbin, D.: Detection of GTA welding quality and disturbance factors with spectral signal of arc light. *J. Mater. Process. Technol.* **209**, 4867–4873 (2009)
- Pal, S.; Pal, S.K.; Samantaray, A.K.: Artificial neural network modeling of weld joint strength prediction of a pulsed metal inert gas welding process using arc signals. *J. Mater. Process. Technol.* **2**(02), 464–474 (2008)
- Acherjee, B.; Mondal, S.; Tudu, B.; Misra, D.: Application of artificial neural network for predicting weld quality in laser transmission welding of thermoplastics. *J. Appl. Soft Comput.* **11**, 2548–2555 (2011)
- Pal, K.; Bhattacharya, S.; Pal, S.K.: Investigation on arc sound and metal transfer modes for on-line monitoring in pulsed gas metal arc welding. *J. Mater. Process. Technol.* **210**, 1397–1410 (2010)
- Cayo, E.H.; Alfaro, S.C.A.: A non-intrusive GMA welding process quality monitoring system using acoustic sensing. *J. Sens.* **9**, 7150–7166 (2009)
- Saini, D.; Floyd, S.: An investigation of gas metal arc welding sound signature for online quality monitoring. *Weld. Res. Suppl.* **77**(4), 172–179 (1998)
- Chen, W.; Chin, B.A.: Monitoring joint penetration using infrared sensing techniques. *Weld. J.* **69**, 181–185 (1992)
- Nagarajan, S.; Banerjee, P.; Chen, W.; Chin, B.A.: Control of the welding process using Infrared Sensors. *IEEE Trans. Robot. Autom.* **8**(1), 86–93 (1992)
- Wikle Iii, H.C.; Zee, R.H.; Chin, B.A.: A sensing system for weld process control. *J. Mater. Process. Technol.* **89–90**, 254–259 (1999)
- Fan, H.; Ravala, N.K.; Wikle, H.C.; Chin, B.A.: Low-cost infrared sensing system for monitoring the welding. *J. Mater. Process. Technol.* **140**, 668–675 (2003)
- Sforza, P.; Blasiis, D.: On-line optical monitoring system for arc welding. *Int. J. Non Destr. Test. Eval.* **35**, 37–43 (2002)
- Ling, S.F.; Wan, L.X.; Wong, Y.R.; Li, D.N.: Input electrical impedance as quality monitoring signature for characterizing resistance spot welding. *Int. J. Non Destr. Test. Eval.* **43**(3), 200–205 (2010)
- Ling, S.F.; Luan, J.; Li, X.; Ang, W.L.Y.: Input electrical impedance as signature for non-destructive evaluation of weld quality during ultrasonic welding of plastics. *Int. J. Non Destr. Test. Eval.* **39**, 13–18 (2006)
- Wu, C.S.; Gao, J.Q.; Hu, J.K.: Real-time sensing and monitoring in robotic gas metal arc welding. *J. Phys.* **18**, 303–310 (2007)
- Wang, Y.; Chen, Q.: On-line quality monitoring in plasma-arc welding. *J. Mater. Process. Technol.* **120**, 270–274 (2001)
- Kang, M. J.; Rhee, S.: The Statistical Models for Estimating the Amount of Spatter in the Short Circuit Transfer Mode of GMAW. *Welding Research Supplement*. Sponsored by the American Welding Society and the Welding Research Council, pp. 1–8 (2001)
- McJunkin, T.R.; Kunerth, D.C.; Nichol, C.I.; Todorov, E.; Levesque, S.: Towards real time diagnostics of hybrid welding laser/GMAW. In: 40<sup>th</sup> Annual Review of Progress in Quantitative Non destructive Evaluation (2014). doi:10.1063/1.4865029
- Nilsiam, Y.; Haselhuhn, A.; Wijnen, B.; Sanders, P.; Pearce, J.M.: Integrated voltage–current monitoring and control of gas metal arc weld magnetic ball-jointed open source 3-D printer. *Machines* **3**(4), 339–351 (2015). doi:10.3390/machines3040339
- Pinar, A.; Wijnen, B.; Anzalone, G.C.; Havens, T.C.; Sanders, P.G.; Pearce, J.M.: Low-cost open-source voltage and current monitor for gas metal arc weld 3D printing. *J. Sens.* (2015). doi:10.1155/2015/876714
- Anzehae, M.M.; Haeri, M.: Welding current and arc voltage control in a GMAW process using ARMarkov based MPC. *Control Eng. Pract.* **19**, 1408–1422 (2011)
- Mollada, J.; Carús, J.L.; Usamentiaga, R.; García, D.F.; Granda, J.C.; Rendueles, J.L.: A fast and robust decision support system for in-line quality assessment of resistance seam welds in the steel-making industry. *J. Comput. Ind.* **63**, 222–230 (2012)
- SatheeshKumar, K.V.; Gejendhiran, S.; Prasath, M.: Comparative investigation of mechanical properties in GMAW/GTAW for various shielding gas compositions. *Mater. Manuf. Process.* **29**(8), 996–1003 (2013)
- Zhang, Z.; Chen, X.; Chen, H.; Zhong, J.; Chen, S.: Online welding quality monitoring based on feature extraction of arc voltage signal. *Int. J. Adv. Manuf. Technol.* **70**(9–12), 1661–1671 (2014)
- Adolfsson, S.; Bahrami, A.; Bolmsjo, G.; Claesson, I.: On-line quality monitoring in short-circuit gas metal arc welding. *Weld. Res. Suppl.* **78**, 59–73 (1999)
- Rehfeldt, D.: Monitoring and analyzing systems for arc welding processes. *JOM-1 (Join. Met.)* 331–335 (1981)
- Rehfeldt, D.; Bollmann, A.: Using statistical signal analysis for analyzing and monitoring GMAW-processes. In: *IIV Latin American Regional Welding Congress (IIV Congreso Regional Latino Americano de Soldagem)*, vol. 2, pp. 839–844. Rio de Janeiro, Brasil (1992)
- Rehfeldt, D.; Schmitz, T.H.: A system for process quality evaluation in GMAW. *Weld. World* **34**, 227–334 (1994)
- Rehfeldt, D.; Polte, T.; Franzbecker, H.; Lübbers, R.; Rostek, W.: Application potential of gas-shielded metal-arc welding with a strip electrode. *Weld. Cut.* **6**, 299–303 (2002)
- Rehfeldt, D.; Rehfeldt, M.D.: Computer-aided quality assurance (CAQ) of Al-MIG-welding with analysator hanover. In: *Proceedings of International Forum on Automobile Welding* (2003)
- Rehfeldt, D.; Rehfeldt, Markus D.: Statistical evaluation of GMAW process disturbances with signature analysis through Analysator Hannover. *J. Chem. Pharm. Sci.* **9**, 274–279 (2015)
- Wu, C.S.; Hu, Q.X.; Sun, J.S.; Polte, T.; Rehfeldt, D.: Intelligent monitoring and recognition of short-circuiting gas-metal arc welding process. *Proc. Inst. Mech. Eng.* **218**(9), 1145–1151 (2004). doi:10.1243/0954405041897121
- Wu, C.S.; Polte, T.; Rehfeldt, D.: A fuzzy logic system for process monitoring and quality evaluation in GMAW. *Weld. Res. Suppl.* **2**, 33–38 (2001)
- Wu, C.S.; Polte, T.; Rehfeldt, D.: GMAW process monitoring and quality evaluation using neural network. *Sci. Technol. Weld. Join.* **5**(5), 324–328 (2000)
- Kumar, V.; Albert, S.K.; Chandrasekhar, N.; Jayapandian, J.; Venkatesan, M.V.: Performance analysis of arc welding parameters using self organizing maps and probability density distributions. In: *IEEE First International Conference on Control, Measurement and Instrumentation (CMI)*, pp. 196–200 (2016)

